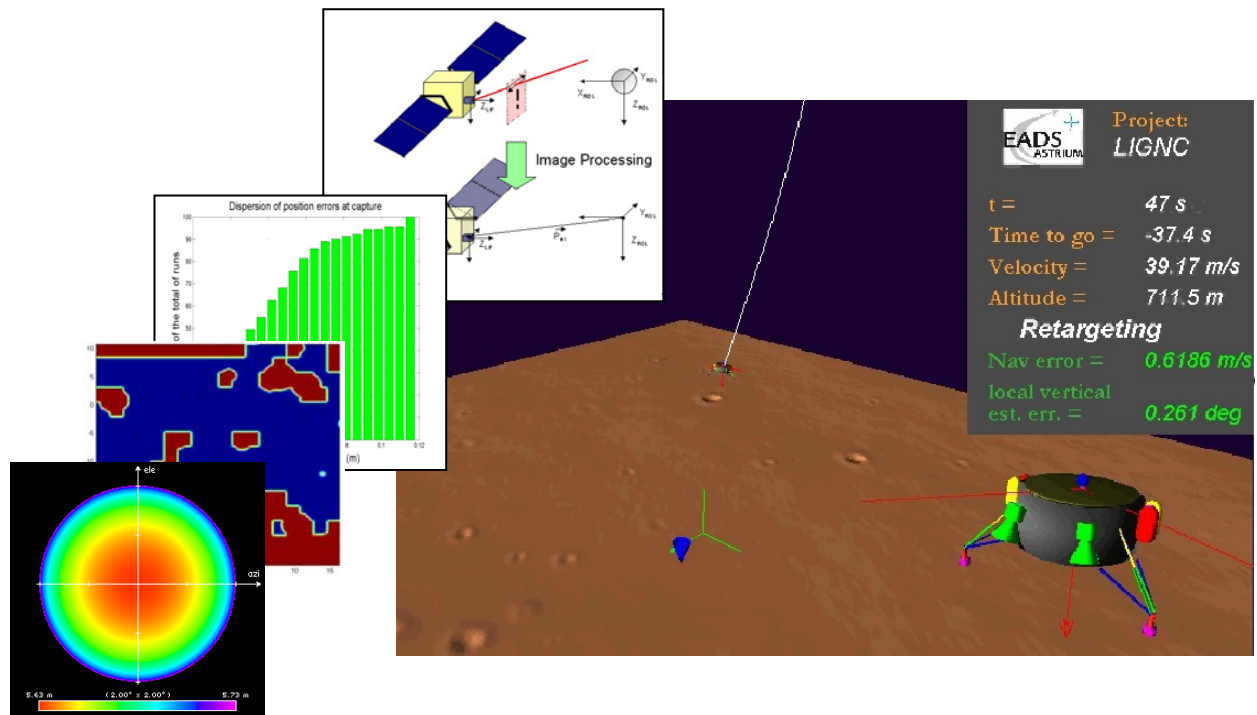
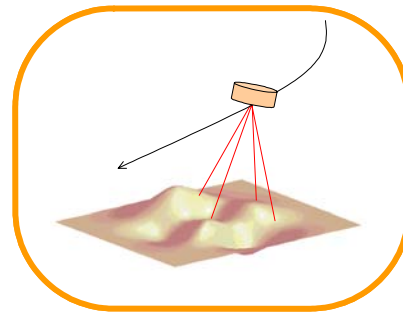
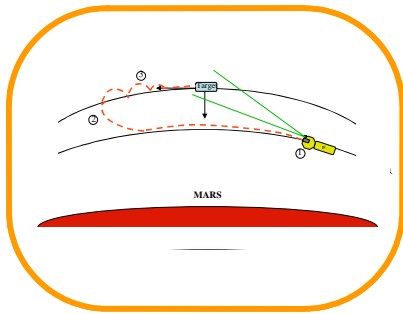


Title

# LiGNC Summary Report



Prepared by	Verified by	Keywords
Xavier SEMBELY	Sébastien BOULADE	LIDAR, GNC, Rendezvous.

---

## ABSTRACT

The “LIDAR-based GN&C for Automatic Rendezvous and Safe Landing” (LIGNC) study is a technological study of the Aurora program, which evaluates the interest of LIDAR technology for supporting soft landing and automatic Rendezvous. The LiGNC study’s objective was to build complete GNC solutions making the most out of the LIDAR capacity. Scanning LIDAR (Laser Imaging Detection and Ranging) is a technology that is now usually used for terrestrial applications to produce 3D mapping of a scene, and which should be soon available for space applications. In particular, this technology could support planetary exploration through its possible application to Soft Landing GNC and Rendezvous GNC, two domains that are both necessary for a Mars Sample Return mission.

Both application cases have been studied with an extensive use of simulation to consolidate the GN&C concepts and assess the associated performances. Two simulation tools have been developed, the RFES (Rendezvous Functional Engineering Simulator) for the Rendezvous application, and the LFES (Landing Functional Engineering Simulator) for the landing application. Both simulators include environment and dynamics models, as well as a LIDAR simulator, generating representative 3D images of the observed scene.

### **GNC DESIGN FOR RENDEZVOUS**

The reference mission here is the scenario of the RVE, envisaged onboard ExoMars to prepare the future MSR mission: a rendezvous in a circular Martian orbit at 550 km of altitude, between a passive canister, a 20-cm-diameter ball and the Martian orbiter.

Capturing a passive canister does not impose too much constraints on the chaser as there is no relative attitude specification nor stringent tracking specifications, as for a docking rendezvous to a space station. The use of a LIDAR further simplifies the design, as it provides almost instantaneously a 3D measure of the relative position. Taking into considerations the above remarks, the proposed GNC was designed in order to gain simplicity while keeping the best robustness to uncertainties. Performances were consolidated, and sensitivity analyses were performed showing the impact of the most important design parameters

### **GNC DESIGN FOR LANDING**

The envisaged scenario was a Martian Landing of a 400-kg platform using propulsion for soft and safe landing. The propulsion system consisted in 4 main engines of 500 N each plus 12 thrusters in 4 clusters for attitude control. The objective was to perform a safe landing; this not only means to estimate the vehicle’s state with respect to the terrain, in particular velocities, but also to generate 3D maps of the terrain, identify the hazards, and decide in real-time and autonomously which landing site to select accounting for both GNC constraints and detected hazards.

A high-performance GNC system was designed and validated taking advantage of EADS Astrium’s long experience in landing GNC analyses and of innovative ideas which allowed solving all the challenges imposed by safe landing.

DOCUMENT CHANGE LOG

<b>Issue #</b>	<b>Date</b>	<b>Modified pages</b>	<b>Observations</b>
1	02/06/03	All	First official issue
2	03/06/03	2	A more complete abstract was added

---

## REFERENCE DOCUMENTS

- [1] “*Statement of Work – LIDAR Based GN&C for Automatic Rendezvous and Safe Landing*”, ESTEC, ref: TOS-ESN/DF/20020826, October 2002.
- [2] Proposal “*LIDAR-based GN&C for Automatic Rendezvous and Safe Landing*”, Astrium ref. SE13.PC.VC.7608.03 , January 2002
- 

## ACRONYMS

FDIR	Failure Detection, Isolation & Recovery
FOV	Field Of View
FOR	Field Of Regard
GNC	Guidance Navigation & Control
IMU	Inertial Measurement Unit
LBNAT	LIDAR-Based Navigation Analysis Tool
LIDAR	Laser Imaging Detection and Ranging
MBTL	Modified Bilinear Tangent Law
MIB	Minimum Impulse Bit
N/A	Not Applicable
NPAL	Navigation for Planetary Approach and Landing
OBC	On-Board Computer
FRES	Rendezvous Functional Engineering Simulator
RVE	RendezVous Experiment
S/C	Spacecraft
VBNAT	Vision-Based Navigation Analysis Tool

## TABLE OF CONTENTS

<b>1</b>	<b>INTRODUCTION .....</b>	<b>6</b>
<b>2</b>	<b>LIDAR-BASED GNC FOR AUTOMATIC RENDEZVOUS .....</b>	<b>8</b>
2.1	REFERENCE SCENARIO .....	8
2.2	RENDEZVOUS LIDAR INSTRUMENT DEFINITION .....	8
2.3	DEVELOPMENT OF A SIMULATION TOOL FOR RENDEZVOUS : THE RFES .....	10
2.4	SYSTEM-LEVEL RESULTS .....	12
2.5	GNC ALGORITHM DESIGN AND PERFORMANCES.....	13
<b>3</b>	<b>LIDAR-BASED GNC FOR SAFE LANDING.....</b>	<b>18</b>
3.1	REFERENCE SCENARIO .....	18
3.2	LANDING LIDAR INSTRUMENT DEFINITION .....	21
3.3	THE SIMULATION TOOL FOR LANDING: THE LBNAT .....	22
3.4	GNC DESIGN AND PERFORMANCES .....	24
<b>4</b>	<b>CONCLUSION.....</b>	<b>31</b>

## 1 INTRODUCTION

The “LIDAR-based GN&C for Automatic Rendezvous and Safe Landing” study was performed from September 2003 to June 2005 by an industrial team lead by EADS Astrium SAS, with University of Dundee, DEIMOS ENGENHARIA, INETI (LAER) and SOLSCIENTIA LDA as subcontractors.

The objective was to study the benefits of using a LIDAR instrument for autonomous GNC in the frame of the Aurora program. The study included two separate topics, which have been developed almost in parallel and independently: Rendezvous in Martian orbit and Landing to Mars.

### Rendezvous mission:

The rendezvous in Martian orbit is one of the most critical phases of the Mars Sample Return Scenario. Because of the long distance between Earth and Mars, it cannot be monitored directly from the Earth, but the operations, especially those at the terminal phase of the Rendezvous, must be entirely autonomous and thus automatic.

The demonstration of this critical phase was therefore also part of the Exomars Mission definition, as studied in Phase A by two industrial teams, one of them being lead by EADS Astrium. The Rendezvous Experiment (RVE) was therefore carefully studied during the ExoMars phase A study, and included some of the results output by the LIGNC study at GNC level.

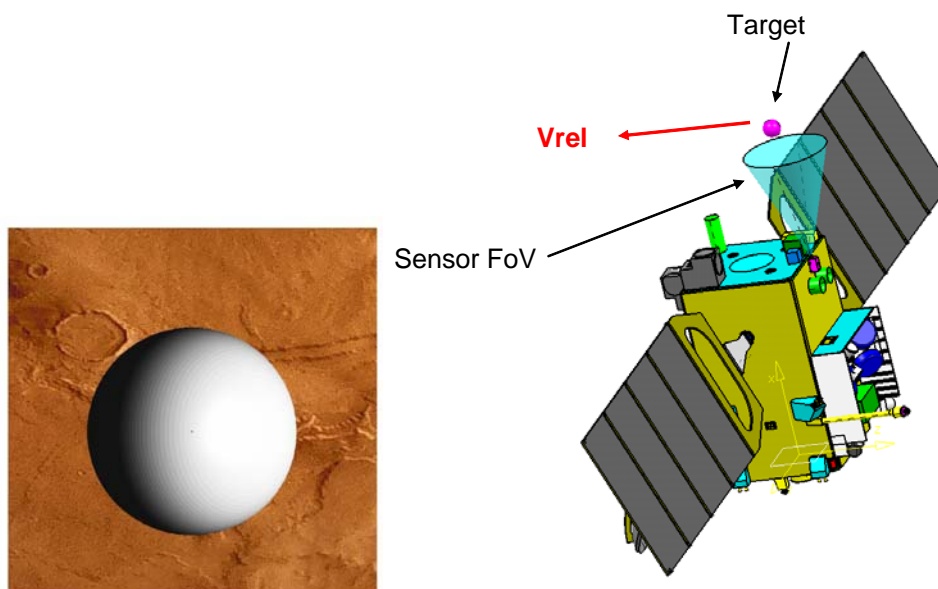
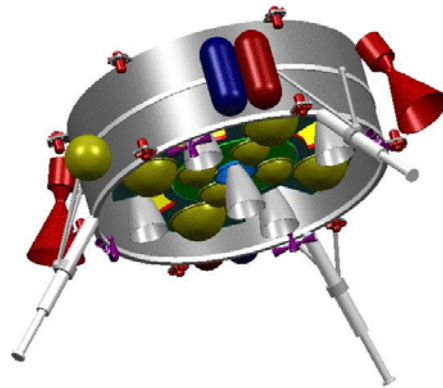


Figure 1: The Rendezvous Experiment as proposed by Astrium for ExoMars: camera image for close distance monitoring and view of the orbiter with the canister.

### Safe Landing on Mars

While the airbag-assisted landing concept reaches its limit as the payload becomes heavier and complex, it was necessary to study in detail the Landing GNC based on a final powered phase for a safe landing approach. Such a controlled landing in a region of high scientific interest (and consequently possibly with

relief) requires to detect hazards, and to have a GNC that guarantee safe landing through hazard avoidance manoeuvres. Here again, the Mars Sample Return mission was the preferred target mission for the study of such a GNC.



**Figure 2: Early design of MSR taken in reference for the LiGNC study**

**Study logic**

These two separate topics can be seen in the study logic, as shown in the figures below, where most of the workpackages were duplicated between Landing and Rendezvous. Among the technical workpackages, the only ones in common concern the LIDAR instrument itself, which share a lot of commonalities between its two applications, Landing and Rendezvous.

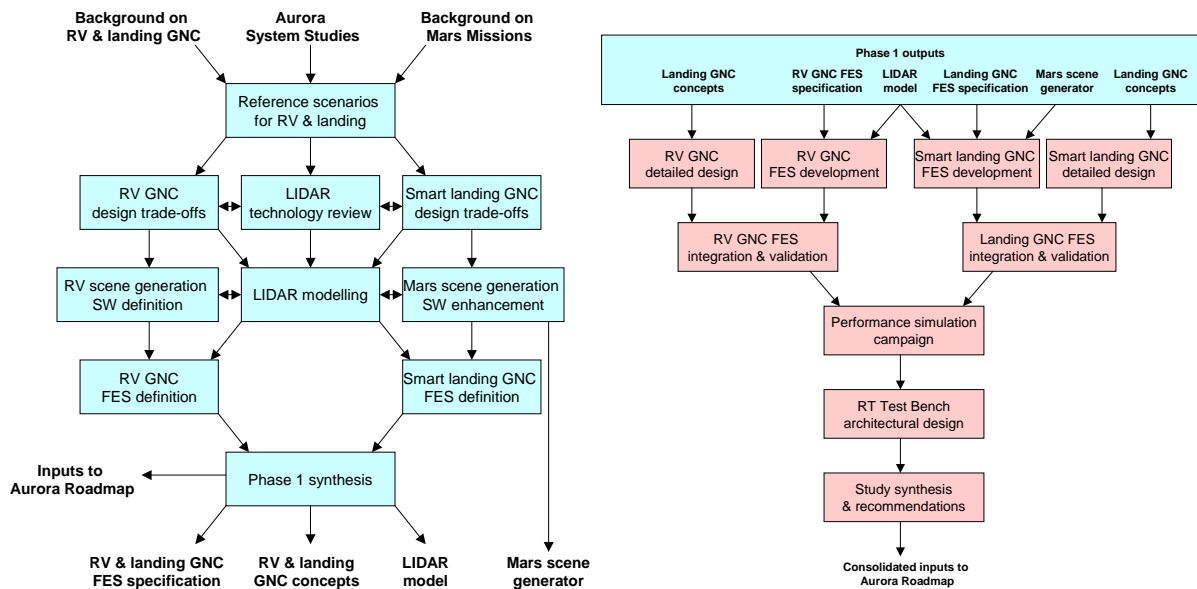


**Figure 3 & Figure 4: Phase 1 & Phase 2 study logic**

The role of the phase 1 was to study the LIDAR instrument and to define the architecture and algorithms, of the GNC and the simulation tools. The phase 2 consisted mainly in the development/coding of the different elements for the simulation, and the assessment of performances through simulations.

## 2 LIDAR-BASED GNC FOR AUTOMATIC RENDEZVOUS

### 2.1 REFERENCE SCENARIO

The reference scenario for this part of the study is an automatic Rendezvous in Martian orbit, between an orbiter and a passive canister. The canister, which would have been launched to orbit by the Mars Ascent Vehicle in the MSR scenario, is supposed to lay on a circular orbit at 550 km of altitude.

The reference scenario deals with capture of a spherical canister, to be distinguished from docking, as the canister is passive and non cooperating. The baseline scenario includes an initial approach on a co-elliptical orbit, then a homing manoeuvre, followed by a set of Vbar hops, down to 100 m of relative distance. The last sequence is a forced translation until contact, but at a low relative velocity.

The LIDAR shall be used for medium and short range approach, i.e. from 5 km to contact. In terms of simulation, it was however decided to focus on the last Station keeping points and the Final translation., the most critical in terms of autonomy of the GNC.

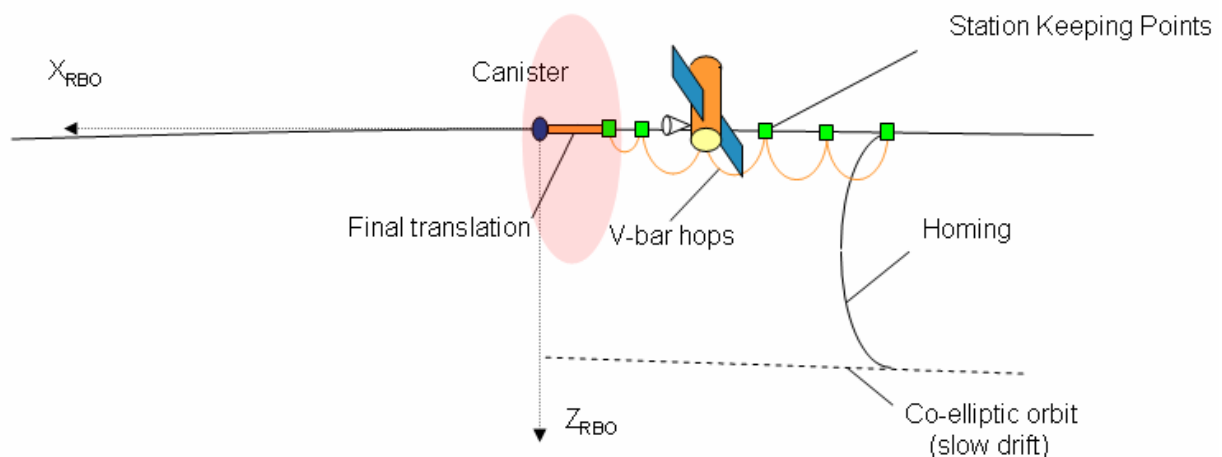


Figure 5: Rendezvous scenario

### 2.2 RENDEZVOUS LIDAR INSTRUMENT DEFINITION

#### 2.2.1 Functional LIDAR specification

One of the first tasks of the study consisted in proposing a set of consistent functional requirements for the LIDAR instrument, and also accounting with the technology capability and limitations.

Although the simulation aspects focused on the last translation, the functional needs had to cover the whole sequence where the LIDAR is to be used.

The resulting functional needs were summarised in the following table:

Item	Value	Unit	Comment
<b>Common parameters for all phases</b>			
Field of view	20 x 20	Degrees	
Azimuth and Elevation accuracy (3 $\sigma$ )	0.02 0.35	Degrees mrad	
<b>Acquisition phase</b>			
Instrument FOV coverage	Full (20 x 20)	deg	
Pixel resolution	0.1 x 0.1	Degrees	
Minimum measurement frequency	0.01	Hz	Higher frequency would improve the performance
Maximum range of operation	5,000	m	Longer range should be preferable
Range accuracy (3 $\sigma$ )	1	m	
<b>Long distance tracking phase</b>			
Instrument FOV coverage	Partial (2 x 2)	deg	But this zone is chosen anywhere in the instrument Field of View
Pixel resolution	0.1 x 0.1	Degrees	
Minimum measurement frequency	1	Hz	
Maximum range of operation	5,000	m	Longer range should be preferable
Range accuracy (3 $\sigma$ )	R*1E-3	m	
<b>Close distance tracking phase</b>			
Instrument FOV coverage	Adaptive	deg	Must cover the whole canister
Pixel resolution	Not specified	-	
Centroid determination	0.1 x 0.1	Degrees	Replace the pixel resolution specification
Minimum measurement frequency	1	Hz	
Maximum range of operation	150	m	
Range accuracy (3 $\sigma$ )	2.5	cm	Centre of the Canister

**Table 1: Rendezvous LIDAR functional needs**

### 2.2.2 Baseline instrument definition

The baseline definition of the LIDAR instrument has been consolidated over the phase 1 of the study. The selected instrument for the simulation demonstration has the following characteristics.

- 2-D Scanning LIDAR with a frame rate of 1 Hz
- Laser: q-switched laser with low repetition rate
- Detector: 4Q APD detector (with a 2x2 matrix of detector)
- Field of View (FOV): 20 deg x 20 deg
- Adaptive Field Of Regard (FOR) within the FOV. The scanning amplitude may vary from 2 x 2 deg to 20 x 20 deg, resulting in sparse scanning in the wide FOV case.
- Angular Resolution: 0.1 deg x 0.1 deg
- Range accuracy: 2.5 cm in final approach

These characteristics are not the only one acceptable for the mission, and different instrument concepts could be applicable for this type of mission; among the reasons for choosing this baseline, we could stress that it allows to have very similar instrument concepts for both rendezvous and landing..

A functional sketch of this instrument is represented here below:

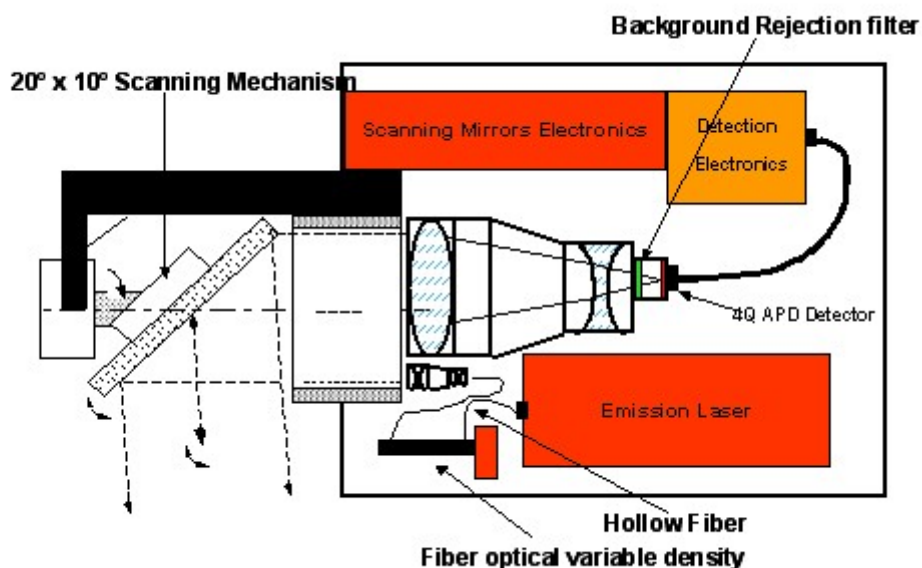


Figure 6: simplified view of the instrument

## 2.3 DEVELOPMENT OF A SIMULATION TOOL FOR RENDEZVOUS : THE RFES

### 2.3.1 Simulation tool

A fine simulation tool has been developed and validated: the RFES (Rendezvous Functional Engineering Simulator)

The simulator, developed with Matlab®/Simulink®, features in particular:

- Dynamics: 6 DOFs for both the canister and the orbiter, orbit propagation, attitude dynamics with wheels (on-board angular momentum), & flexible modes
- Environment: atmospheric drag, sun pressure, Mars gravity model
- Equipment: LIDAR (see next paragraph), but also Propulsion, wheels, Star Tracker, IMU

Moreover the architecture and the management of parameter initialisation and post-processing functions, make the RFES a powerful tool for handling batches of simulation, in particular Monte-Carlo campaigns.

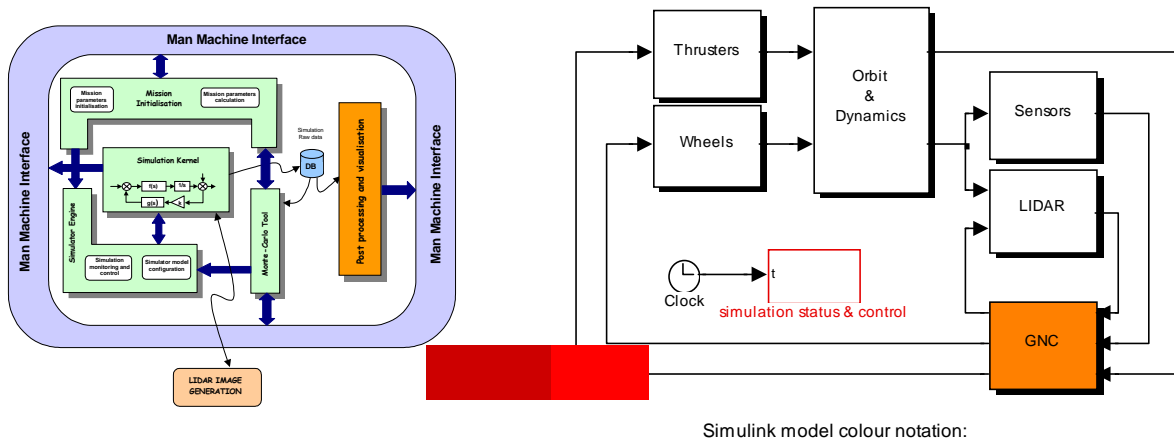


Figure 7: The Rendezvous Functional Engineering Simulator

### 2.3.2 LIDAR model

A particular effort has been spent to create an accurate of the LIDAR model that reproduces with the highest fidelity the physical behaviour of a LIDAR and generate LIDAR images.

This effort has been separated in two main parts, that constitutes the LIDAR model:

- The LIDAR Image Generator, named PANGU, which is an evolution of a software developed originally for synthetic (vision) image generation of Planetary and asteroid surfaces, and also utilised in its visual version during the NPAL<sup>1</sup> study. PANGU generates “perfect” LIDAR images, in the sense that it calculates with all available numerical precision the range, i.e. the distance run by the laser rays at each pulse. This includes also a description of the scanning pattern which is accurately reproduced, taking also into account the true spacecraft motion during the scan. PANGU also generate a specific image for the corner cubes (we will see in section 2.4 that cornercubes are necessary on the canister), which is then mixed to the former one (lambertian) in the Physical LIDAR model. Laser incidence angles on target is also returned by PANGU
- A Physical LIDAR model, which generates all sources of error, pointing errors, range errors, laser echo distortion, and combination of lambertian reflexion image with cornercube reflexion image to create a unique LIDAR image.

<sup>1</sup> “Navigation For Planetary Approach and Landing” ESA Contract 15618/01/NL/FM

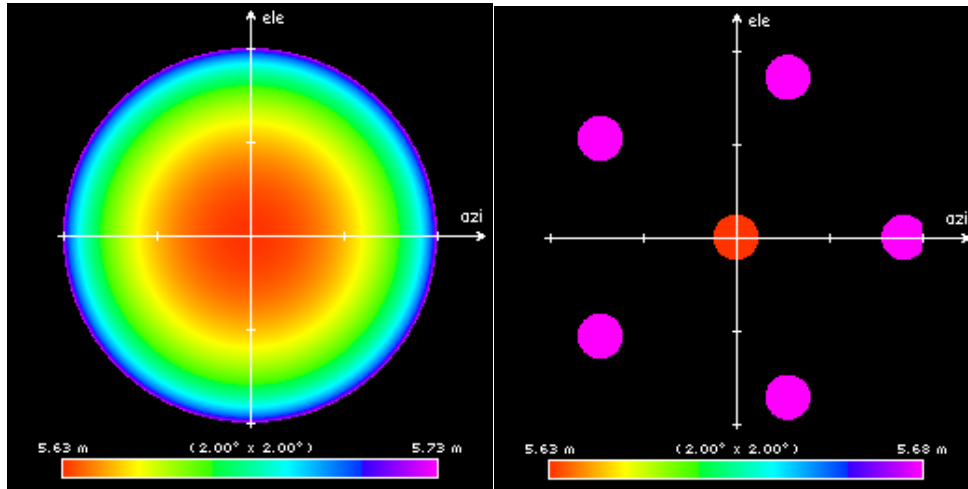


**Figure 8 & Figure 9: Lambertian and cornercubes LIDAR images from the PANGU**

## 2.4 SYSTEM-LEVEL RESULTS

### Long range detection

To meet the requirement of medium range detection – up to 5 km – the power budget of the received light must be carefully managed. It was shown that for such a small target, the only solution for detection at ranges longer than 2 km was to equip the canister with corner cubes.

A configuration for the corner cubes, uniformly spread over the canister surface in an isocahedron configuration, was proposed to be able to be robust to any canister attitude and angular velocity.

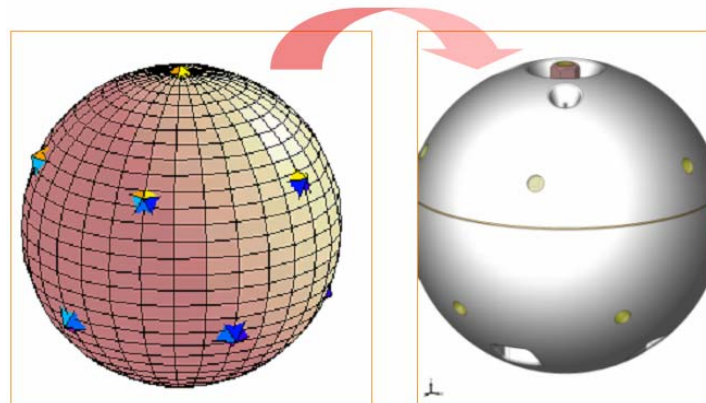


**Figure 10: The isocahedron configuration of the corner cubes proposed by LiGNC was retained for ExoMars (in EADS Astrium’s baseline)**

The above configuration was then retained in baseline by EADS Astrium’s study team for the Exomars Phase A. Of course, we demonstrated in the frame of the study that those corner cubes, necessary for long range detection can be managed at short distance also. In particular that the possible detector saturations can be managed.

**Free-drift sequence**

Having an instrument that has a medium range capacity makes it difficult to also operate at very short range. As a consequence, the LIDAR will stop providing valid measurements at a few meters of distance (typically 2 m). Of course one obvious solution is to rely on an other instrument to monitor the final seconds before capture. An innovative alternative was proposed, where the strategy for the last meters consists in a free-drift, where the propulsion is cut-off, leaving the system uncontrolled. Switching all active systems off is the best option to guarantee the absence of any hazardous event between instrument loss and capture. Starting the free-drift at 5m – with some margins with respect to the measurement loss – enables to verify that the relative kinematics are within specifications (leaving time to trigger an escape manoeuvre if necessary) and was proven to have adequate accuracy, despite residual dispersion. The orbital coupling is such that the free-drift induces a vertical motion of (typically) 20 cm, but this can be anticipated as completely deterministic.

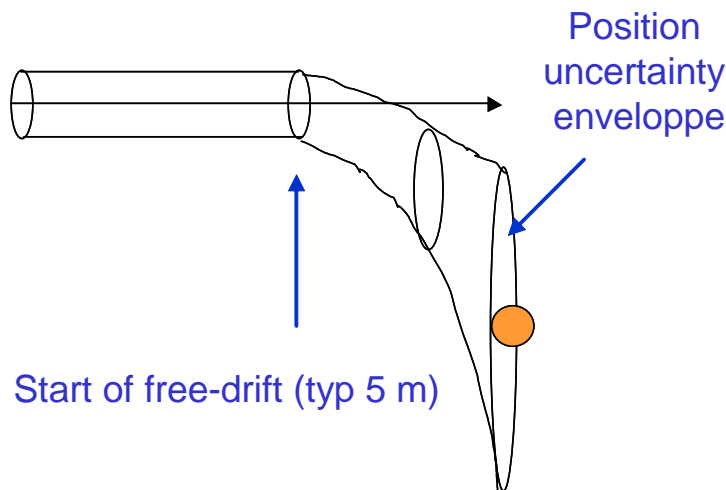


**Figure 11: In absence of other sensor for contact monitoring, a free drift (with no control at all) appeared as the most interesting solution for the last meters**

As a consequence, at system level, this vertical motion shall be anticipated by locating the capture mechanism and the LIDAR instrument in a configuration that is compatible with this scenario.

**2.5 GNC ALGORITHM DESIGN AND PERFORMANCES**

**2.5.1 LIDAR image processing**

The objective of the Image Processing algorithm is to retrieve the 3D relative position of the orbiter with respect to the canister from the LIDAR Range image. It was shown that simplified Image-Processing algorithms are sufficient here, and that the saturation due to cornercubes was easily managed without performance degradation.

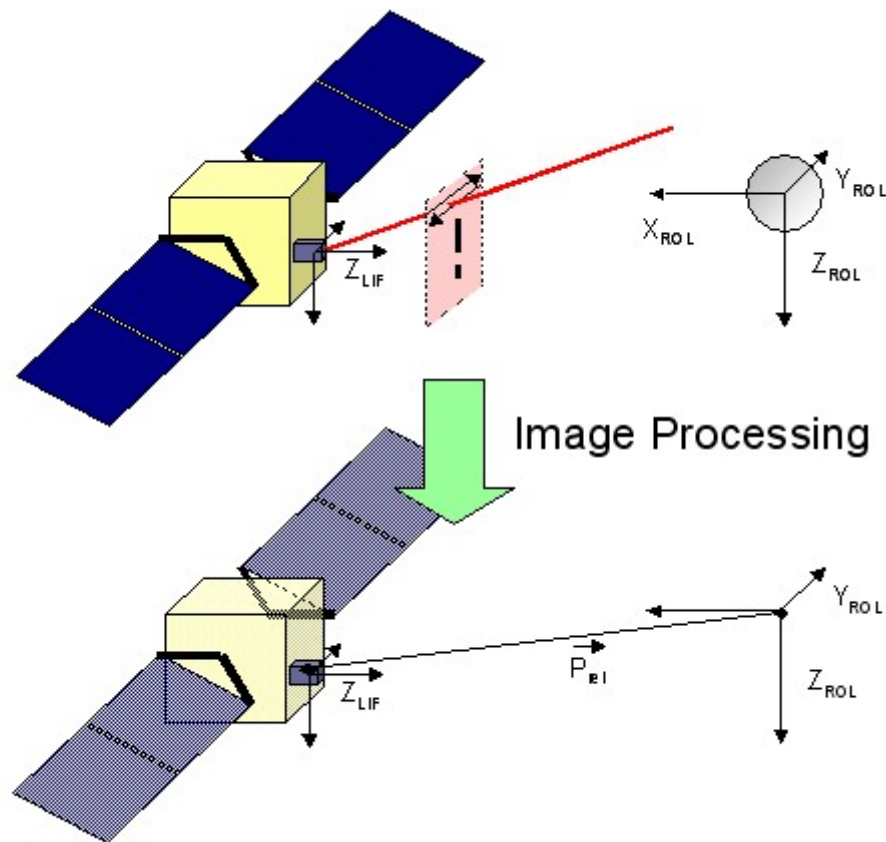


Figure 12: The image processing transforms the LIDAR image in relative position measurement

### 2.5.2 Rendezvous GNC design

A scenario based on « Capture » is much less constraining than docking at GN&C level, and the use of the LIDAR which directly outputs 3D measurements authorise simple design choices:

- **Control** : a decoupled architecture was built, where each of the 6 axis are controlled almost independently.
- **Navigation** : Although the system is by definition a dynamic system (with a relative distance varying between 100 m and 0), a fixed-gain Kalman filter was chosen for navigation, not only on angular axes but also on the translation axes, reducing the complexity (with respect to optimal Kalman filter) while keeping excellent estimation performances.

The whole GNC design was based on circular orbit assumption and linearization, through the classical Clohessy-Whitshire equation, resulting in fully linear and steady state GNC equations.

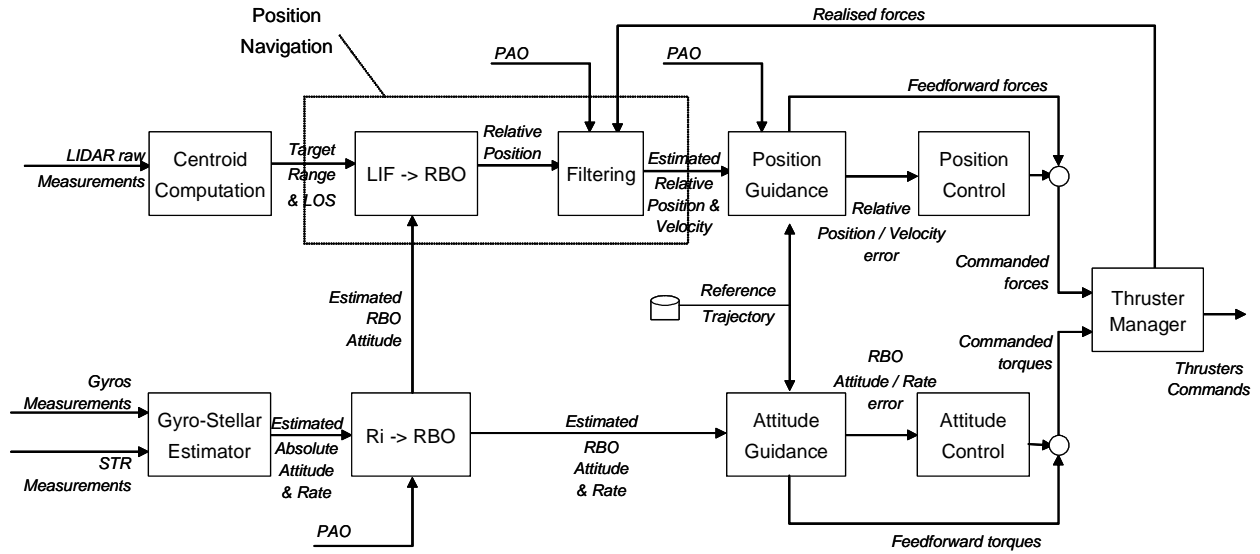


Figure 13: Rendezvous GNC Architecture

2.5.3 Rendezvous GNC performances

Extensive performance Monte-Carlo campaigns have been performed. Capture of the 20-cm-wide canister with an accuracy of less than 12 cm was demonstrated. But the main contributors to these final performances were also established: Performance is driven by the residual velocity at the beginning of free-drift.

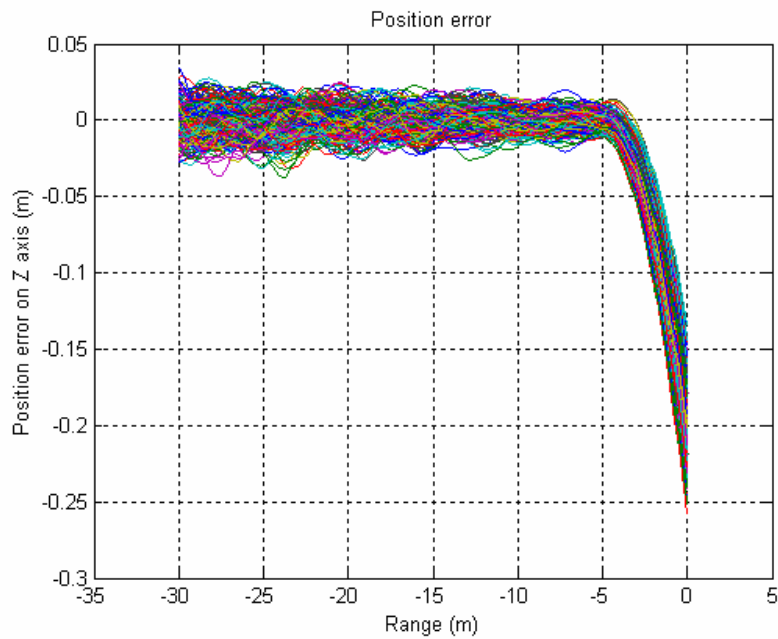
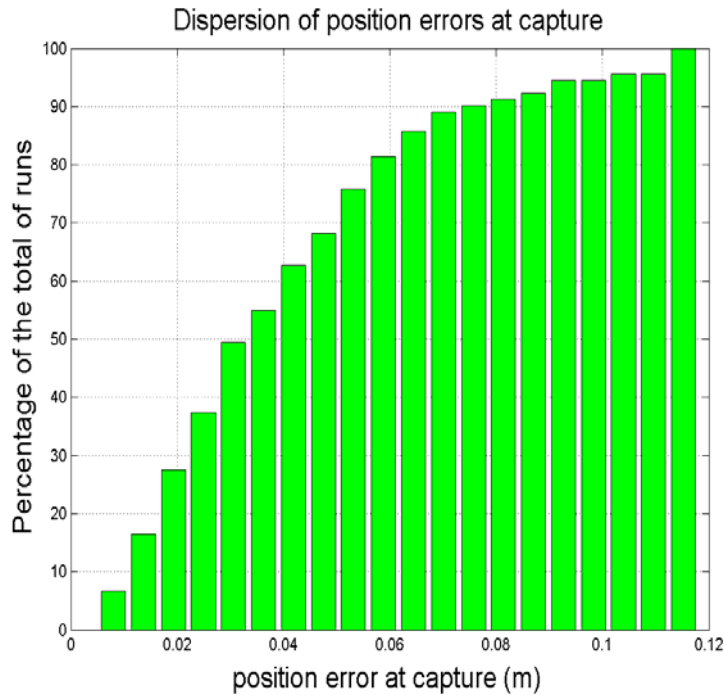


Figure 14: Trajectories of the final approach for a Monte-Carlo campaign



**Figure 15: Capture performance histogram.**  
**The 2- $\sigma$  value (in the sense of 95.6% confidence) is 11 cm.**

Not only were the end-to-end performances established, but some sensitivity analysis and robustness analysis have also been achieved.

The sensitivity campaigns were divided in two groups: the campaigns that dealt with scenario parameters (such as Approach velocity, free-drift distance, or orbit eccentricity) and the campaigns that analysed the influence of LIDAR parameters (FOV, pointing errors). The understanding of the GN&C performances and of its driving parameters was then consolidated.

Name	Description	Nb of Runs	Main Results
CMP1	End-to-end perfo. Station Keeping @ 100 m	100	2- $\sigma$ perfo is 25 cm
CMP2	End-to-end perfo. Station Keeping @ 10 m	100	2- $\sigma$ perfo is 5 cm
CMP3	End-to-end perfo. Final translation	100	2- $\sigma$ perfo is 12 cm at capture
CMP4	Length of free-drift	100	Between 2 and 6m is acceptable
CMP5	Approach velocity	100	Wide domain of approach velocity validated at GNC level

CMP6	Influence of position bandwidth	100	Trade-off between accuracy and fuel consumption
CMP7	Influence of eccentricity	50	Acceptable up to $10^{-3}$
CMP8	Influence of lighting conditions	30	No influence
CMP9	Influence of LIDAR resolution	100	0.1 deg consolidated
CMP10	Influence of mirror jitter	100	Influence is small

**Table 2: Campaign summary**

As an illustration, robustness to residual eccentricity errors was studied with a batch of 50 simulations, reproducing various conditions. The results shows that the concept designed in this study can handle up to  $10^{-4}$  of eccentricity without any impact, and up to  $10^{-3}$  with a small degradation only of performances as presented on the following figure:

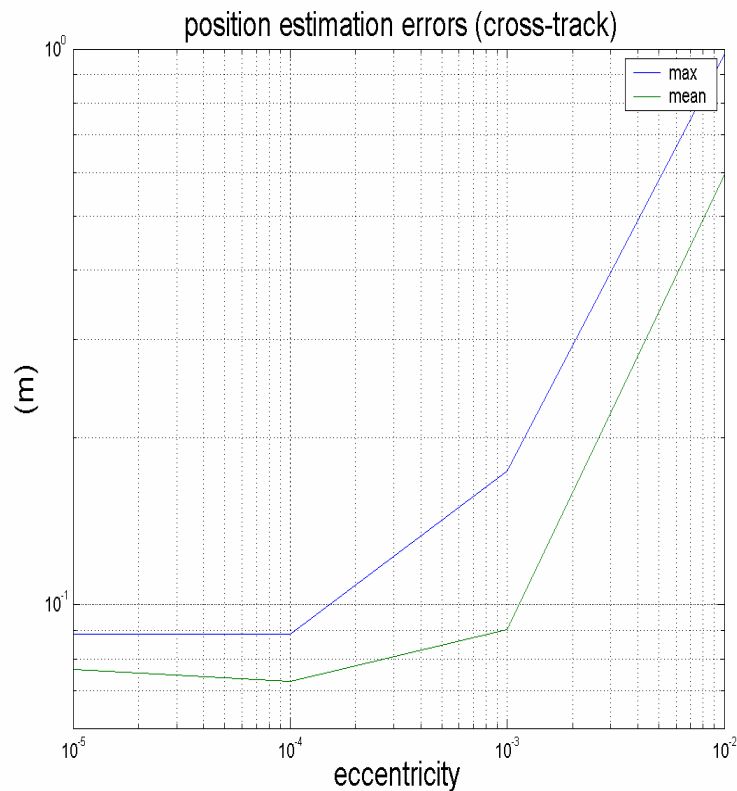


**Figure 16: influence of the eccentricity error on the Position estimation error.  
The GNC is validated for residual eccentricities up to  $10^{-3}$ .**

### 3 LIDAR-BASED GNC FOR SAFE LANDING

#### 3.1 REFERENCE SCENARIO

The scenario taken in reference for this study is inspired from the MSR study. The descent in the Martian atmosphere starts with a ballistic phase with a heatshield, followed by a sequence of deployment and release of one or many parachutes. These early phase are out of the scope of the present study. The first point of interest is the point of first acquisition of Lidar images, typically about 3 to 5 km above the ground. After the jettisoning of the main chute, a powered phase is started at typically 2 km of altitude, which will end with a soft touchdown on the Martian surface, at a velocity of typically 1 m/s, and with the main engines cut-off.

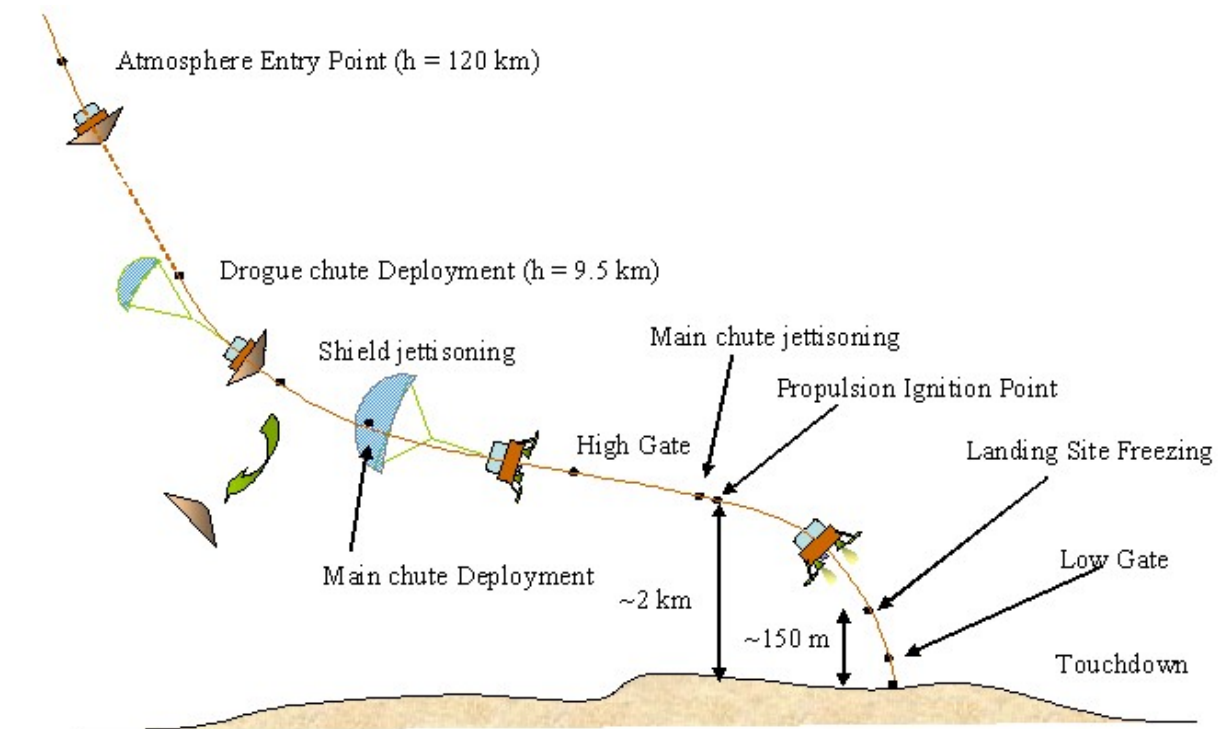
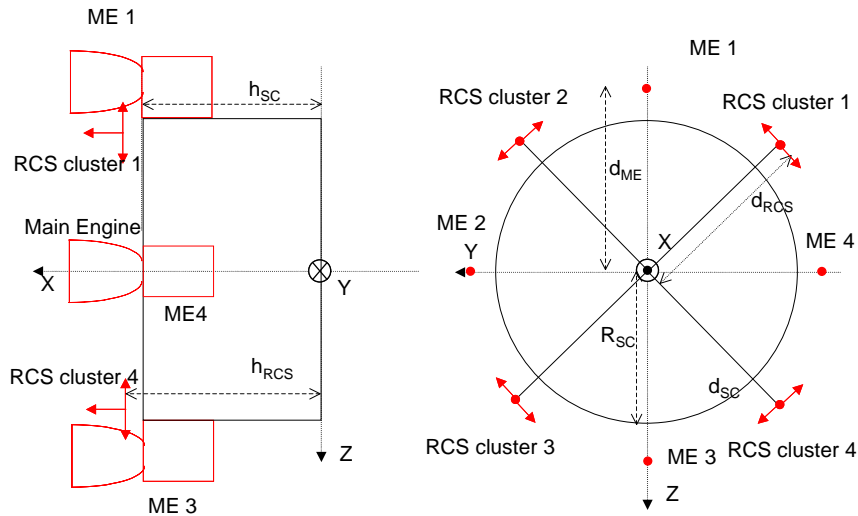


Figure 17: Entry Descent and Landing scenario

The considered lander is about 400 kg with the following propulsion systems:

- Four 500-N Thrusters as main engines (on-off modulation at 1 Hz)
- 12 RCS thrusters operated at 10 Hz for attitude control



**Figure 18: Lander propulsion configuration**

These characteristics were frozen quite early, and consequently they do not exactly correspond to those that were finally retained in baseline neither for Exomars nor MSR at the end of their Phase A. But they present a very consistent set of hypotheses, so that this study represents a good starting point to be re-derived for each candidate mission in the future.

### Safe Landing and hazard avoidance

Previous landing experiences, especially the American probes Surveyor, Viking and Mars Polar Lander (even if the latter has failed) are references of great interest. The new feature that is studied here, is the new concept of « safe landing ». Landing on an unknown terrain such as the Martian surface presents risks, due to presence of boulders of potentially sloppy terrains, which can be minimised by identifying the potential hazards, and perform avoidance manoeuvres.

The implementation of safe landing requires to implement major changes in the GN&C architecture: safe landing constraints prevent from using the reference “gravity-turn” guidance law, implemented in the cited reference missions because of its very limited retargeting capability.

The GN&C architecture shall integrate the constraint of safe landing through the capability to perform hazard mapping, autonomously designate landing sites, and regenerate trajectories a few times over the descent to reach the updated landing target point, as illustrated on the figure below.

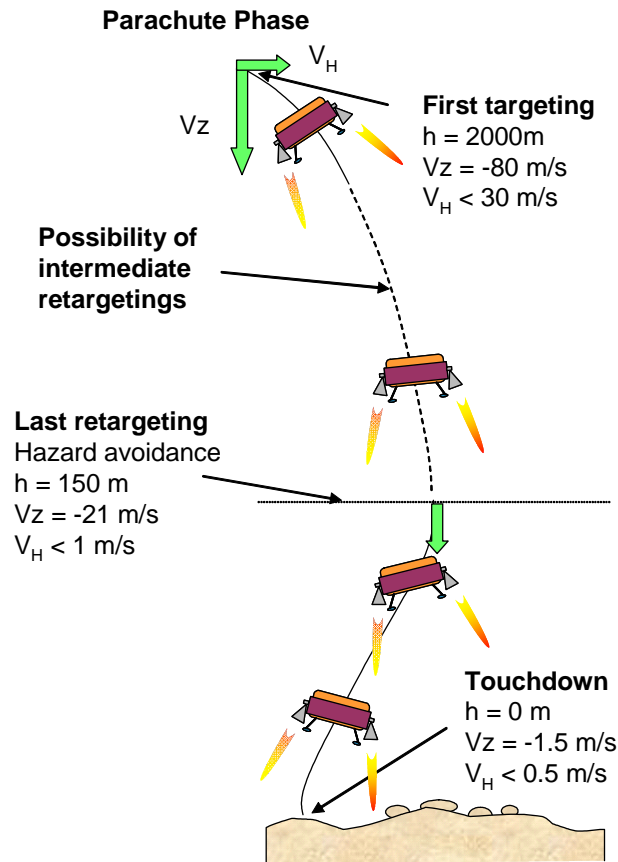


Figure 19:Synopsis of the powered phase

### Landing with a LIDAR

A LIDAR measures the Time Of Flight of the laser light. 3D maps are then produced by 2-D scanning.

But the scanning takes time, typically 1 s, so that LIDAR images are not snapshots, but are distorted by the lander's motion.

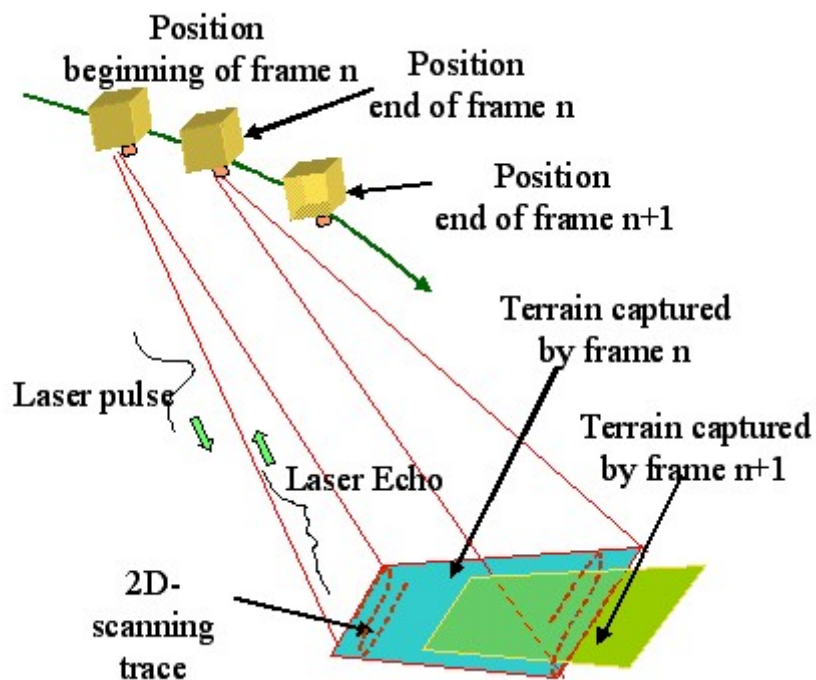


Figure 20: How the LIDAR takes 3D images over the descent

Another challenge is that there alignment of the successive maps is not known a priori. A dedicated algorithm must be implemented to do so. This is, with the hazard mapping, one of the main tasks of the LIDAR Image processing algorithms.

### 3.2 LANDING LIDAR INSTRUMENT DEFINITION

#### 3.2.1 LIDAR functional specifications

The set of functional specifications was also derived for the Landing application. It is summarised in the table below:

Item	Value	Unit	Comment
Field of view	20 x 20	Degrees	
Frame rate	1	Hz	All along the trajectory
Number of pixels per frame	400 x 400	-	The number of laser pulse could be lower, using array detectors
Minimum range of operation	20	m	5 m preferred
Maximum range of operation	3,500	m	5,000 m preferred
Range accuracy (3- $\sigma$ )	0.1	m	@ 300 m of distance
Azimuth and Elevation accuracy (3- $\sigma$ )	0.02	Degrees	
	0.35	mrاد	

**Table 3: Landing LIDAR specifications**

The number of pixels and the FOV are not completely firm specifications. They should be seen as target value, and should be finally chosen as a trade-off between ground resolution, Field of View, and Computational load.

### 3.2.2 Instrument definition

The baseline definition of the LIDAR instrument, consolidated over the phase 1 of the study, is very close to the instrument defined for Rendezvous:

- Scanning LIDAR at 1 Hz
- MultiKhz pulse repetition rate Laser with 1.06 $\mu$ m of wavelength (Yag with AO internal cavity modulation)
- 2-direction scanning
- Detector: 4Q APD detector
- Field of View: 20 deg x 20 deg preferred for good coverage of Martian terrain. Note that the performances demonstrated in simulations correspond to with 10 deg x 10 deg (100 x 100 pixel images).
- Angular Resolution: 0.1 deg x 0.1 deg

The main difference between the instrument defined for Rendezvous and the present instrument concerns the choice of the laser. While the power budget was the main concern in rendezvous, the objective here is to obtain large terrain maps with good resolution, requiring a high repetition rate for the laser (of the order of 10 kHz).

## 3.3 THE SIMULATION TOOL FOR LANDING: THE LBNAT

### 3.3.1 Simulation core

Instead of developing a new simulator from scratch, EADS Astrium has chosen to rely on a family of simulation tools, dedicated to powered landing.

The VBNAT, Vision-Based Navigation Tool, developed in the frame of the NPAL project for landing on non atmospheric planets (e.g. Mercury), was adapted in the frame of LIGNC.

The adaptations concerned mainly the modelling of the interactions with the atmosphere, and the replacement of NPAL's camera model by a LIDAR model, including the PANGU which generates “perfect” LIDAR images and a physical model, which adds various effects, distortion, noise, etc, according to the instrument physics.

Of course, the GN&C design was also largely modified with respect to NPAL, although it served as starting point, at all levels Guidance, Navigation and Control.

With this approach, it was possible to have very quickly a mature and reliable simulator to develop advanced GN&C concepts.

This tool also proved to be able to handle hundreds of simulation in Monte-Carlo campaigns and in sensitivity analyses.

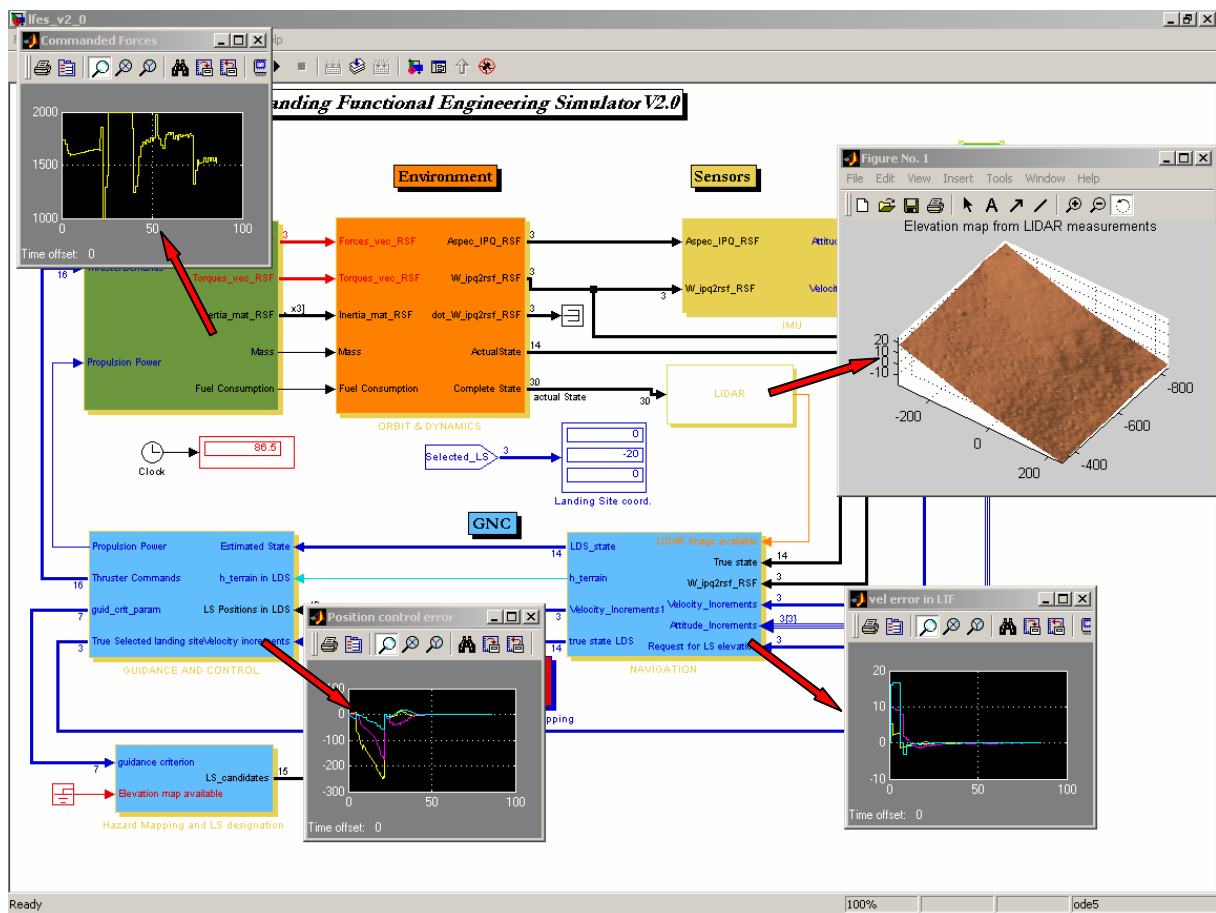
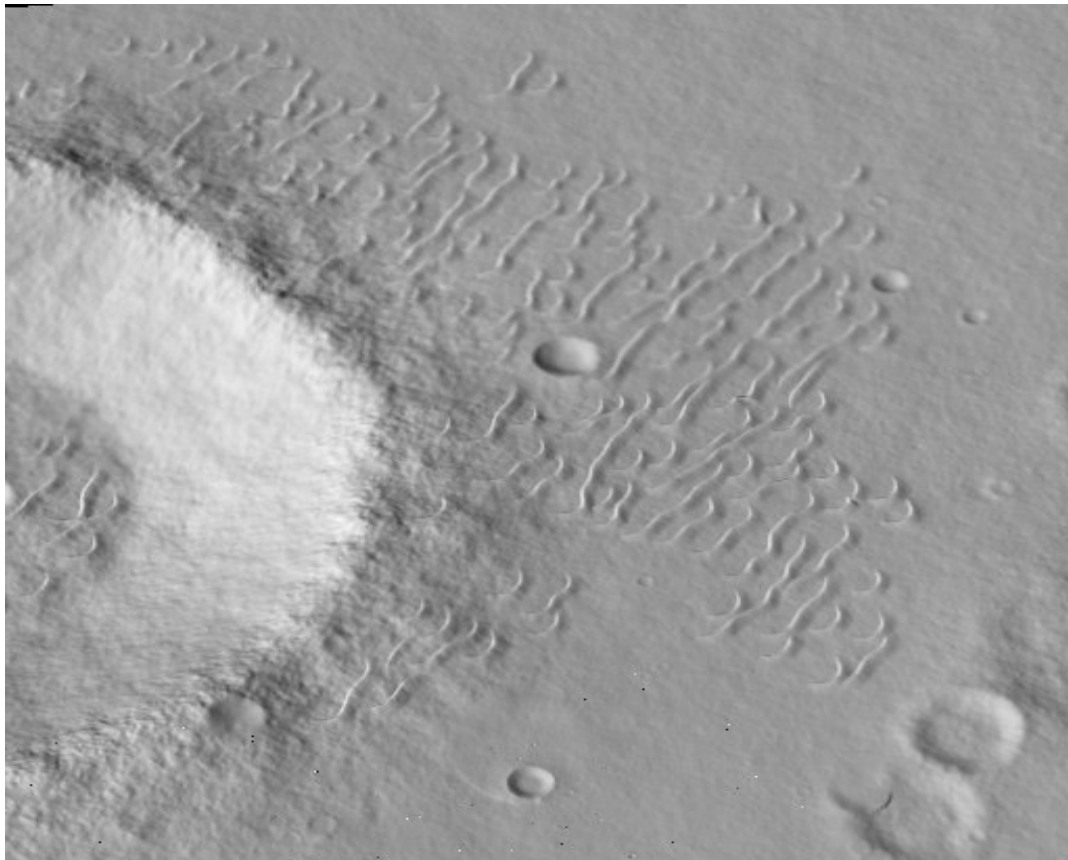


Figure 21: The LBNAT (Lidar-Based Navigation Analysis Tool) is derived from NPAL's VBNAT. The simulator itself is also referred as the LFES (Landing Functional Engineering Simulator)

### 3.3.2 LIDAR model

The approach for modelling the LIDAR instrument was strictly identical to the one described for the Rendezvous application, of course without the presence of corner cubes which simplifies the model.

A specific effort has been spent to the PANGU so that the synthetic scenes are as representative as possible to real Martian terrains.



**Figure 22: Visualisation of typical synthetic terrain generated by PANGU**

With respect to previous PANGU developments, new developments have included in particular the possibility to use the MOLA data as starting terrain, and to add structures such as sand dunes.

## 3.4 GNC DESIGN AND PERFORMANCES

### 3.4.1 Overview of the Landing achievements

A landing GN&C design is very challenging, because it is a very constrained GNC problem:

- About 1 minute to estimate vehicle states, designate a landing site, and control the vehicle in a large domain of dynamic conditions.
- Technology limitations: LIDAR scan time (typ. 1 s) and propulsion on-off modulation frequency (10 Hz max)

The proposed GNC design fulfills those challenges, with an innovative guidance law well-adapted to retargetings, with a navigation design based on LIDAR image correlation, with a control characterised by a metric accuracy, and by a full tolerance to wind gusts (up to 15 m/s), and with an autonomous safe Landing site designation capability.

A typical simulation output is shown here below:

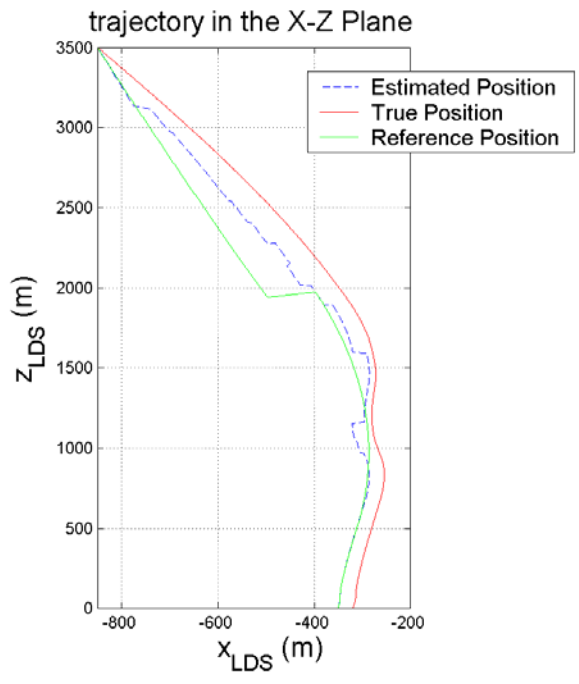


Figure 23: Powered descent trajectory

The avoidance manoeuvres can be seen on this figure (the most visible is triggered at 1000 m of altitude for instance). The reader shall notice that the estimated position does not exactly converge to the true trajectory. This is because the absolute position is simply not observable. However, velocity with respect to the terrain and the attitude angles (2 axes angles defining the local vertical) are fully observable, as shown on the figures below:

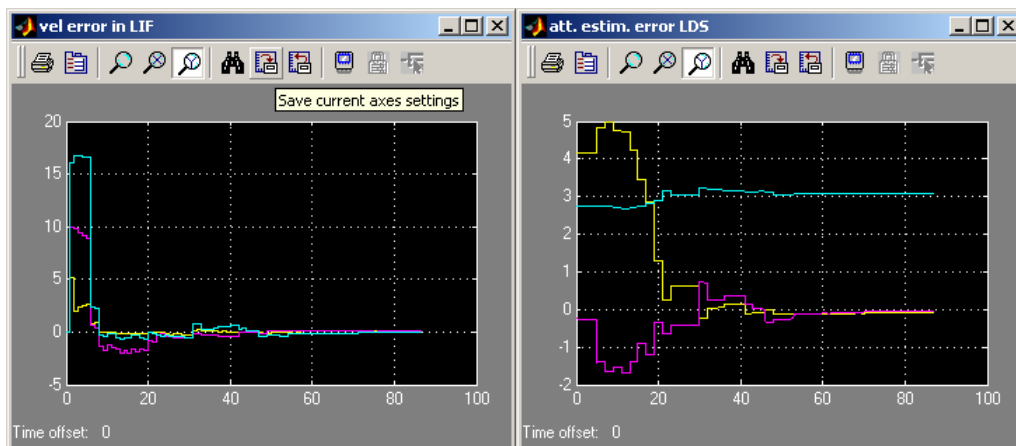
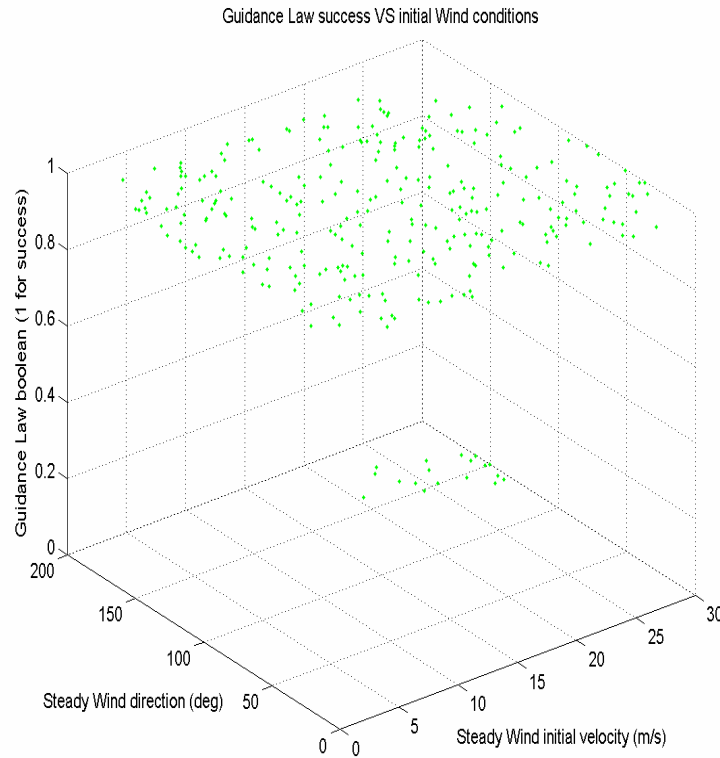


Figure 24 & Figure 25: Convergence of the estimation errors (velocity, attitude)

### 3.4.2 Guidance

An innovative guidance law has been designed, based on previous experience (internal development, Lunar Landing in the 90s, and more recently NPAL): the Modified Bilinear Tangeant Law (MBTL).

The capability of the MBTL to regenerate trajectories in real-time during the descent was demonstrated, and Monte-Carlo campaigns have proved the tolerance to wind conditions to a value as high as 30 m/s.



**Figure 26: The guidance always converges except in the zone of very unfavourable winds, due to thrusters saturation.**

Landing site designation has been successfully implemented. It chooses the best landing site according to:

- Simplified guidance criterion
- Surface roughness, i.e. presence of boulders
- Minimum surface slope

The simplified criterion was developed to include guidance in the selection process, while minimizing the associated computation load for the On-Board Computer. These three separate criteria are mitigated to produce Hazard maps. A typical hazard map is presented below for a typical terrain full of boulders.

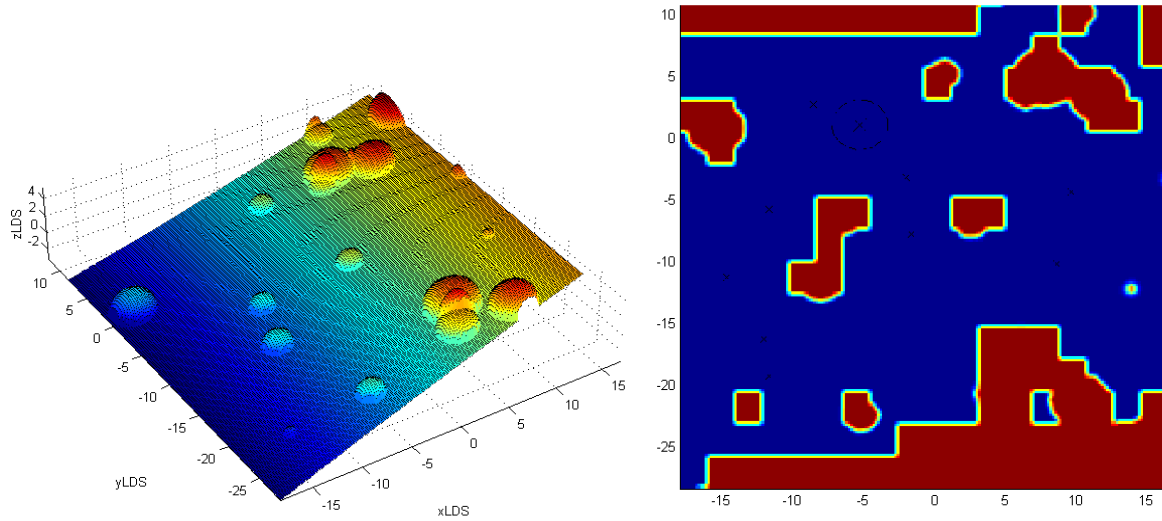


**Figure 27 & Figure 28: Elevation map and its corresponding hazard map**

The operation of the whole guidance chain, including simplified guidance criterion, hazard mapping, landing site designation, trajectory generation, and, on top of them, the guidance management module, was validated in Monte-Carlo campaigns. In the illustration below, 20 out of the batch of simulation have been represented, with the last terrain map, and the last selected landing site.

Landing site designation in the terrain maps (20 simulations)

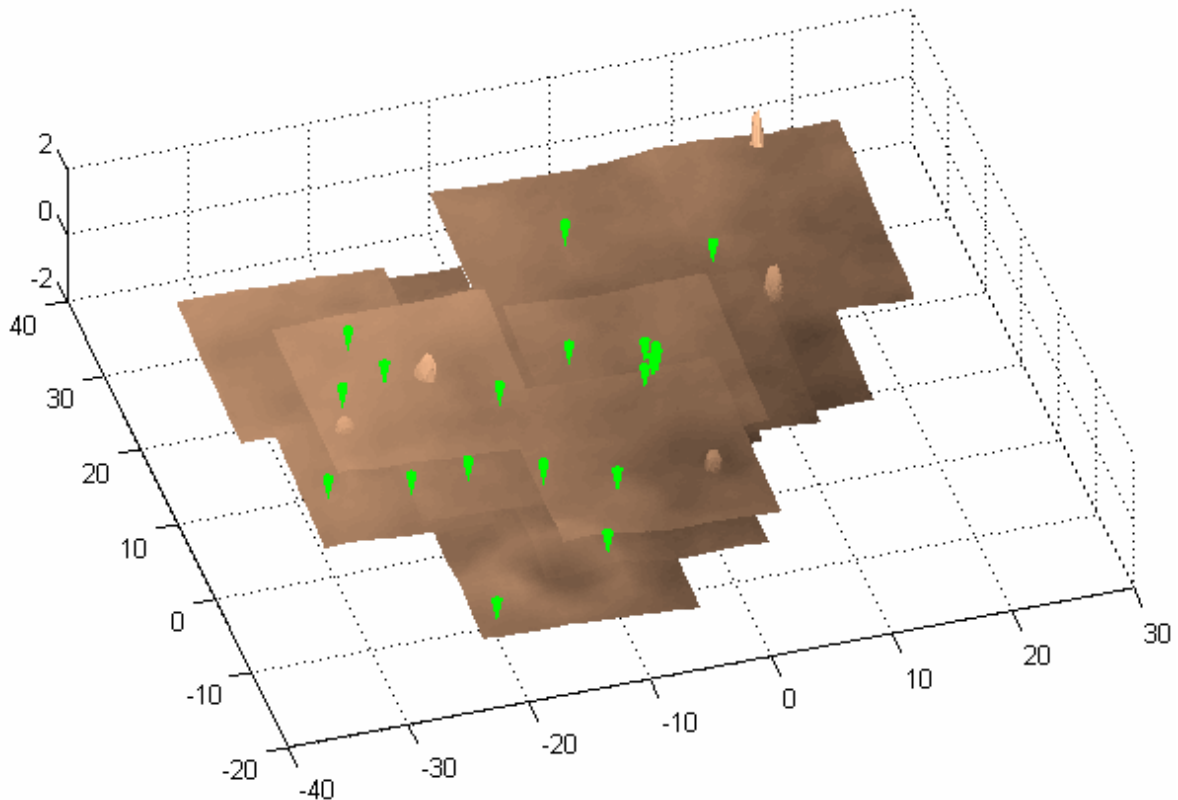


**Figure 29: Selected landing sites within their elevation maps for 20 runs of the Monte-Carlo campaign**

### 3.4.3 Control

The control architecture relies on nested trajectory and attitude control loops: as the thrusters are fixed in the spacecraft frame, the trajectory control requires pointing the whole vehicle in order to point the Force vector in a given direction.

The challenge of this control design, based on SISO control, was therefore to demonstrate that it worked despite the large vehicle manoeuvres involved (up to 40 degrees). The control design for this highly non-linear dynamic system was implemented and validated.

Performances were assessed with a Monte-Carlo campaign dedicated to Control, and in the same time, robustness to gust of winds was demonstrated, up to 15 m/s.

Finally it was shown that the control errors remain always smaller than 1 m.

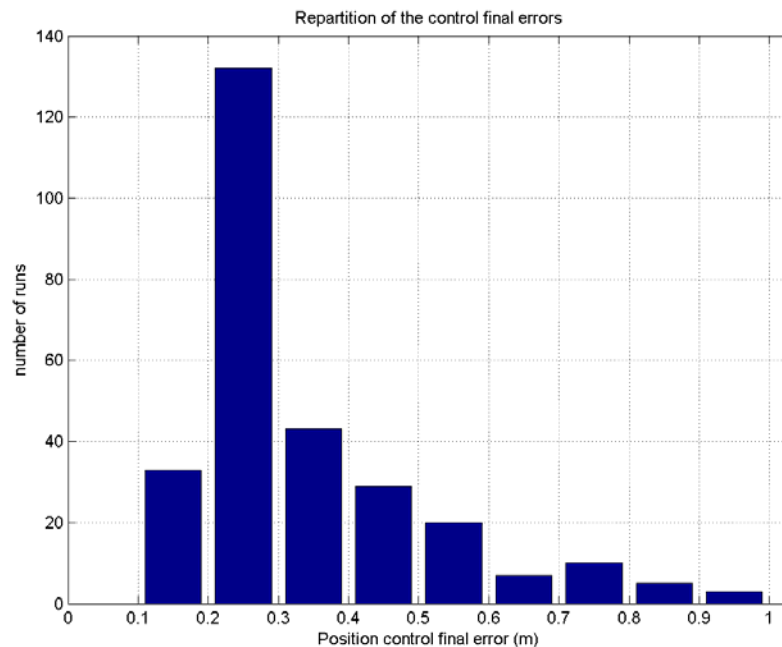
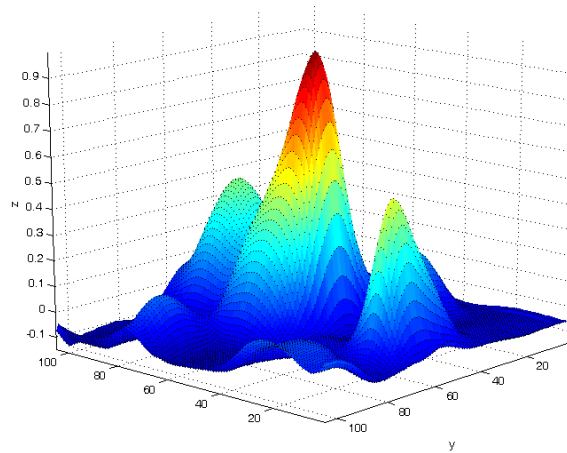


Figure 30: Control performance at touchdown is always smaller than 1 m.

### 3.4.4 Navigation

The main design choice for the navigation consisted in correlating the successive 3D images to output an estimate of the velocity with respect to the ground, and then in designing the navigation filter as if the instrument was simply a velocity instrument.

The image processing mostly consisted in the compensation of the spacecraft motion during the scan, map resampling and correlation of pairs of images using the normalized cross-correlation.



**Figure 31: Correlation function**

Locating the correlation peak as seen on the figure above enables to define the displacement between two images and thus the velocity.

The concept based on LIDAR image correlation turned out to be extremely efficient. Not only the velocity with respect to the terrain can be measured, but also the attitude, or at least the two angles defining the direction of the local vertical.

The implementation of the navigation filter relied on the core Extended Kalman Filter that has been developed along years through a long experience of EADS Astrium in the domain, and in particular it re-used the core functions of NPAL's filter.

The demonstrated performances in Monte-Carlo were beyond expectations: 100% of convergence has been demonstrated over a wide domain of initial uncertainty – up to 30 m/s in velocity, and up to 15 deg in attitude.

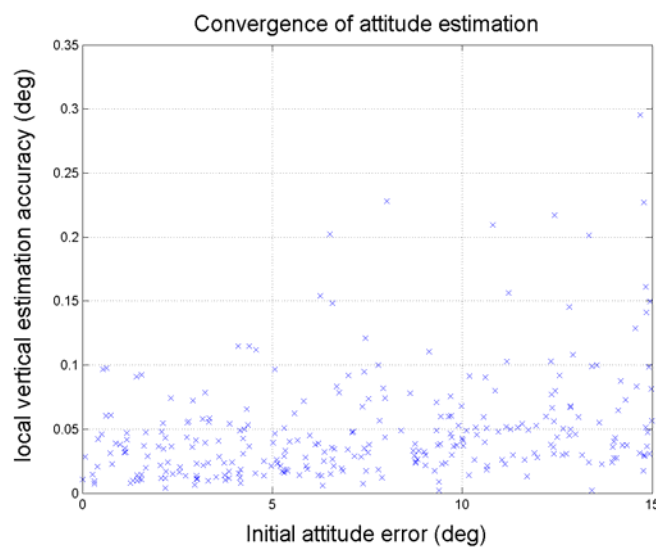


**Figure 32: Attitude convergence as a function of the initial attitude estimation error**

Moreover the converged performances of the filter reach an accuracy of 20 cm/s in velocity and 0.2 deg in local vertical estimation.

Such excellent results could have very positive impact at system level. For instance, it could be possible not to propagate the attitude during re-entry (case of a ballistic re-entry), removing some cost-driving functional needs, such as the need for additional star sensor to initialise the attitude before re-entry, or a for high-grade IMU to propagate it (Note that a low-grade IMU is still required).

### 3.4.5 Overview of the performances campaign

10 performances campaigns were performed on Landing. They are summarised here below:

Name	Description	Nb of Runs	Main Results
CMP1	Guidance & Control Performance demonstration	300	Full validation of G&C
CMP2	NAV: Sensitivity to LIDAR resolution	315	Direct dependence demonstrated
CMP3	NAV: performances with simplified LIDAR	300	2- $\sigma$ perfo is 0.25 m/s
CMP4	NAV: End-to-end performances	100	2- $\sigma$ perfo is 0.20 m/s
CMP5	End-to-end simulation	1	For illustration mainly
CMP6	Performances of the Hazard Mapping	40	HM integration demonstrated
CMP7	Influence of number of retargetings	300	3 retargeting selected
CMP8	Test of retargeting strategies	300	Several strategies acceptable
CMP9	Influence of LIDAR FOV for initial convergence	100	Convergence guaranteed even for small FOV
CMP10	Influence of LIDAR FOV for final retargeting	100	Small FOV do not prevent successful landing

**Table 4: Landing campaign summary**

Most of the main results have been illustrated in the previous sections.

## 4 CONCLUSION

### LIDAR definition

At instrument level, the LIGNC study achieved to:

- Consolidate the functional needs of a LIDAR instrument for the considered application
- Propose a baseline definition of the instrument
- Develop a fine model of the LIDAR instrument, including PANGU and a physical model for that baseline, and that can be easily adapted to any preferred definition.

### GNC achievements

The demonstration of the GNC performances was fully successful in both the Landing and the Rendezvous application.

In rendezvous, the GNC design was simple and robust, thanks to the relaxed constraints of capture with respect to docking, and the accuracy at contact should be of the order of 10 cm.

In Landing, the challenging GNC design demonstrated performances beyond expectations, in terms of tolerance to initial uncertainties in particular.

### Beyond LIDAR

The LIGNC study was the opportunity to master the GNC techniques beyond the LIDAR-related aspects, in particular in the landing application.

In both applications one of the major achievements was the construction of two high-fidelity simulators, which can be re-used for other applications with a minimum of adaptation.

In landing, the developed Guidance and Control algorithms are applicable for any Terrain sensor (LIDAR, Camera, mapping Radar) meeting the navigation requirement. The navigation concepts can be adapted for any sensor measuring the velocity with respect to the terrain, in particular to 4-beam Doppler Radar or Lidar.

### Future work

The next steps forward consists, at GNC level, in consolidating the real-time implementation, and in particular the implementation trade-off for the Image Processing algorithms. At instrument level, it consists in a breadboarding activity.

Finally a full demonstration with a Real-Time Test Bench with hardware in the loop should be envisaged to complete the validation of the concepts.

PAGE IS INTENTIONALLY LEFT BLANK

---

**DISTRIBUTION LIST**

Denis FERTIN	ESA
Gilbert GRISERI	EADS Astrium
Benoit FRAPARD	EADS Astrium
Pascal REGNIER	EADS Astrium
Steve PARKES	Univ of Dundee
Marti DUNSTAN	Univ of Dundee
Bento CORREIA	INETI
Luis PENIN	DEIMOS
David RESENDES	Soscientia
GED	EADS Astrium